UJEAS

UNIZIK JOURNAL OF ENGINEERING AND APPLIED SCIENCES

UNIZIK Journal of Engineering and Applied Sciences 6(2), June (2026), 3487-3501
Journal homepage: https://journals.unizik.edu.ng/index.php/ujeas
PRINT ISSN: 2992-4383 || ONLINE ISSN: 2992-4391

Boundary-Mediated Phase Ordering and Collision-Free Dynamics in a Vibro-Impact Multi-Particle System

Nicholas N. Topman
Department of Mathematics, Enugu State University of Science and Technology (ESUT), Enugu, Nigeria
Email: topman.nnamani@esut.edu.ng

Abstract
This study investigates a mechanically realizable vibro-impact system exhibiting collision-free multi-particle motion under boundary-induced excitation. The system consists of identical spherical particles undergoing one-dimensional ballistic motion under gravity and repeated impacts with a structured vibrating boundary. While individual particles obey identical free-flight and restitution laws, experiments reveal the spontaneous emergence of temporally ordered, collision-free motion when multiple particles interact with a common impulsive base. To explain this behavior, a minimal non-smooth dynamical model is formulated using Newtonian mechanics and impact-based boundary conditions. The governing equations define an event-driven discrete impact map advancing the system between successive collisions. Although no explicit inter-particle forces are introduced, collective dynamics arise through boundary-mediated timing regulation. Under bounded excitation, the discrete update preserves temporal separation, suppresses synchronous impacts, and stabilizes staggered impact sequences as attracting configurations. The formulation extends classical single-particle bouncing-ball theory to a multi-particle setting and demonstrates how structured boundary excitation induces phase ordering in non-smooth impact systems. Numerical simulations and controlled laboratory measurements confirm the theoretical predictions. The results provide a dynamical explanation of collision-free behavior in vibro-impact systems and establish a framework for boundary-induced regulation in multi-particle impact dynamics.

Keywords: Collision-free dynamics, Vibro-impact systems, Non-smooth dynamical systems, Impact dynamics, Phase ordering, Mechanical vibration

1. Introduction

Vibro-impact systems constitute a fundamental class of non-smooth dynamical systems in which continuous motion is intermittently interrupted by instantaneous impacts. The classical bouncing-ball problem, describing a particle interacting with a vertically vibrating boundary, has long served as a canonical model for impact-driven nonlinear dynamics. Early analytical investigations demonstrated that repeated impacts with a periodically excited surface generate periodic motion, chattering, bifurcations, and chaotic regimes depending on excitation parameters and restitution properties (Holmes, 1982; Luck and Mehta, 1993). Complementary theoretical and pedagogical analyses further clarified the mechanisms governing these behaviors (Chastaing et al., 2015; Dorbolo et al., 2005). Subsequent refinements established discrete impact maps as a natural mathematical framework for describing such systems and analyzing their stability properties (Barroso et al., 2009; Luo and Han, 1996). Beyond deterministic periodic forcing, stochastic excitation and energy injection mechanisms have also been investigated. Randomly driven bouncing-ball systems were shown to exhibit nontrivial power-injection statistics and transitions between ordered and irregular motion (García-Cid et al., 2015; Giusepponi et al., 2005).

The influence of restitution, dissipation, finite contact duration, and impact chattering on long-term dynamics was systematically examined, revealing strong sensitivity to boundary excitation characteristics (Giusepponi and Marchesoni, 2003; Luo and Zhu, 2024). Extensions incorporating fractional damping and generalized dissipation mechanisms further enriched the analytical understanding of vibro-impact stability and bifurcation structure (Xie et al., 2022). Collectively, these studies established vibro-impact oscillators as archetypal models for analyzing non-smooth nonlinear phenomena.

Modern developments have significantly expanded vibro-impact theory through advanced stability diagnostics and global discrete-map techniques. Non-autonomous and non-harmonic excitation strategies were shown to substantially influence periodic and chaotic impact regimes (Lampart and Zapoměl, 2016; Torres and Núñez, 2009). Computer-assisted global analysis and reduced smooth map approaches have enabled rigorous exploration of complex impact dynamics (Bao et al., 2025), while nonlinear energy sink concepts have been employed to investigate targeted energy transfer and multi-state responses in vibro-impact configurations (Liu et al., 2023; Youssef et al., 2025). Experimental and computational analyses of higher degree of freedom impact systems revealed complex resonance structures, period-doubling cascades, and multi-attractor behavior (Fritzkowski and Awrejcewicz, 2021; Yan et al., 2025). Vibro-impact-based vibration mitigation strategies have likewise been examined in engineering contexts (Veltman et al., 2025; Dekemele and Habib, 2025). These advances underscore the rich nonlinear structure inherent in impact-driven systems and highlight the decisive role of boundary excitation in shaping global stability.

Parallel to these theoretical advances, vibration-induced transport and granular handling have attracted sustained attention in engineering applications. Vibratory platforms can induce pumping, directed transport, and fluidization of particulate materials, with relevance to material processing and micro-mechanical devices (Adachi et al., 2024; Adhikari et al., 2024). Granular flows over vibrated bases demonstrate that excitation parameters influence collective transport efficiency and structural ordering (Sonar et al., 2024), while comprehensive reviews confirm that forcing geometry critically affects granular dynamics (Watson et al., 2023). Experimental rigs incorporating impact constraints and structured boundaries further illustrate how surface configuration modifies vibro-impact dynamics and directional drift behavior (Zhang et al., 2024).

However, as particle populations increase, conventional vibration-driven systems frequently exhibit clustering, repeated collisions, and degradation of temporal ordering. Recent experimental efforts have therefore explored structured surfaces and tailored excitation protocols as mechanisms for regulating granular motion. Dynamic manipulation of dry friction and boundary geometry has been shown to influence transport efficiency and mitigate undesired interactions under specific operating conditions (El Banna et al., 2026). Nevertheless, most existing multi-particle vibratory studies rely primarily on empirical observations or numerical simulations. A predictive analytical framework capable of explaining stable impact-suppressed multi-particle motion under impulsive excitation while remaining consistent with experimental measurements remains limited.

From a nonlinear-dynamical standpoint, most vibro-impact models address single-degree of freedom oscillators, nonlinear energy sink configurations, or explicitly coupled systems (Herisanu et al., 2023; Li et al., 2025). Multi-state similarity analyses and harmonic excitation studies confirm that collective responses typically arise through direct mechanical coupling mechanisms (Gong et al., 2024; Pagano et al., 2024). Even in sophisticated multi-modal systems exhibiting internal nonlinear interactions and intermodal energy exchange (Weidemann et al., 2025; Gzal et al., 2024), temporal organization is generally mediated by physical interconnections rather than purely boundary-induced effects. Far less attention has been devoted to multi-particle systems in which temporal ordering emerges solely through interaction with a shared vibrating boundary and without explicit inter-particle forces. In particular, the question of how collision-free motion and persistent phase separation can arise among multiple identical particles interacting only through a common vibrating platform remains largely unexplored. Classical bouncing-ball theory treats particles independently (Barroso et al., 2009), while granular transport models frequently assume collision-dominated dynamics (Sonar et al., 2024). The emergence of ordered temporally separated configurations within a shared impact environment.

Therefore, represents a distinct nonlinear phenomenon requiring dedicated analysis. The present framework differs fundamentally from conventional bouncing-ball and granular vibro-impact formulations in both mechanism and dynamical interpretation. Classical impact oscillator models primarily describe isolated particle dynamics or systems involving explicit inter-particle coupling. In contrast, the current study demonstrates that stable collision-free collective motion may emerge solely through boundary-mediated timing regulation, without requiring direct contact forces between particles. The proposed discrete non-smooth formulation therefore introduces a new synchronization mechanism in which the vibrating boundary itself acts as a phase-ordering regulator. This establishes a distinct nonlinear dynamical regime extending beyond traditional single-particle impact theory and conventional collision-dominated granular transport models.

Motivated by this gap, the present study develops a combined mathematical and experimental framework for collision-free multi-particle vibro-impact dynamics on a vertically excited, radially structured platform. Experiments reveal that multiple identical spherical particles spontaneously self-organize into temporally staggered trajectories characterized by sustained temporal ordering and suppression of inter-particle collisions, despite the absence of direct contact forces. To interpret this behavior, we formulate a minimal impact-driven model in which each particle obeys identical one-dimensional ballistic motion under gravity and restitution-based impact laws. The governing equations naturally define an event-driven discrete map advancing the system from one impact to the next (Luo and Han, 1996).

Although no explicit inter-particle coupling is introduced, the shared boundary induces timing-dependent velocity updates that act as an effective timing-stabilization mechanism. Within this non-smooth discrete framework, synchronous impacts are dynamically unstable, whereas staggered impact sequences form locally attracting configurations. The structured vibrating surface thus functions as a timing regulator that preserves impact separation and suppresses clustering, extending classical single-particle vibro-impact theory to a collective setting governed by boundary-mediated excitation (Holmes, 1982). Unlike classical vibro-impact models that rely on direct inter-particle interactions, this work demonstrates that purely boundary-induced timing regulation is sufficient to generate stable impact-regulated multi-particle dynamics, establishing a new mechanism for temporal self-organization in non-smooth systems.

1.1 Main Contributions

The principal contributions of this study are as follows:

- Development of a boundary-mediated dynamical framework demonstrating that collision-free multi-particle motion can arise without explicit inter-particle forces.
- Identification of temporal self-organization as an emergent property of non-smooth impact dynamics governed by shared boundary excitation.
- Formulation of an event-driven discrete model combining gravitational motion, restitution-based impacts, and excitation-induced timing regulation.
- Stability characterization showing that staggered impact sequences form attracting configurations, while synchronous impacts are dynamically unstable.
- Experimental validation demonstrating quantitative agreement with theoretical predictions and confirming sustained collision-free behavior.
- Establishment of design principles for vibration-driven particle transport systems based on boundary-induced timing stabilization.

2. Model Assumptions

The model assumes identical rigid spherical particles undergoing predominantly one-dimensional vertical motion under gravity. Lateral motion is constrained by the radially structured surface. Particle–base interactions are modeled as instantaneous inelastic impacts characterized by a constant restitution coefficient. The vibrating base provides periodic excitation and introduces weak boundary-mediated coupling through shared impact timing. Air resistance, rotational effects, and tangential friction are neglected. These assumptions are consistent with the experimental configuration and are justified by the moderate velocity regime and the constrained particle trajectories observed in laboratory measurements. The neglect of rotational and tangential effects is justified by the predominantly vertical motion observed experimentally and by the constrained trajectories imposed by the radially structured surface geometry

2.1 Governing Equations

The dynamics of the system consist of successive free-flight intervals under gravity interrupted by impulsive interactions with a vertically excited, radially structured base. The governing equations are formulated to reflect both the ballistic motion of individual particles and the boundary-mediated coupling introduced by the shared vibrating platform.

$$m\,\frac{d^2y_i}{dt^2} = -mg \tag{1}$$

From equation (1), we have;

$$\ddot{y}_i = -g \tag{2}$$

where: $y_i(t)$ is the vertical position of particle i, m is the particle mass, g is the gravitational acceleration.

Integrating the equation (2) which is the equation of motion yields the velocity and position of each particle during free flight:

$$\frac{dy_{i(t)}}{dt} = v_i(t) = v_{i,n}^{+} - g(t - t_{i,m}) \tag{3}$$

And

$$y_i(t) = v_i^+{}_{,n}(t - t_{i,n}) - \frac{1}{2}g(t - t_{i,n})^2 \quad (4)$$

where: $t_{i,n}$ is the time of the n^{th}impact of particle i,
$v_i^+{}_{,n}$ is the velocity immediately after the n^{th} impact.
An impact occurs when the particle reaches the base surface, defined by

$$y_i(t) = 0 \quad (5)$$

The velocity immediately before impact is:

$$v_{i,n}^- = \lim_{\tau \to \tau_{i,n}} \frac{dy_i(t)}{dt} \quad (6)$$

The rebound of each particle from the base is modeled using an effective coefficient of restitution e, satisfying $0 < e < 1$
The post-impact velocity is given by;

$$v_i^+{}_{,n} = ev_i^-{}_{,n} + U(t_{i,n}) \quad (7)$$

Where: $ev_i^-{}_{,n}$ is the pre-impact velocity, $v_i^+{}_{,n}$ is the post impact velocity, $U(t_{i,n})$ represents the impulsive excitation provided by the base at time $t_{i,n}$. The term $U(t)$ accounts for energy regulation and phase control induced by the system.
From equation (5) we obtain,

$$y_i\left(t_{i,n_{+1}}\right) = 0 \quad (8)$$

Solving equation (8) we obtain the time interval between two consecutive impacts given as;

$$v_i^+{}_{,n}T_{i,n} - \frac{1}{2}gT_i^2{}_{,n} = 0 \quad (9)$$

The next impact happens when the ball returns to the base when $y = 0$.
Flight time = (time of next impact) − (time of current impact), so we have:

$$T_{i,n} = t_{i,n_{+1}} - t_{i,n} \quad (10)$$

Where $t_{i,n}$ = time when the ball leaves the base, $t_{i,n_{+1}}$ = time when it returns.
When solving motion equations, we describe the position at any time t after the last bounce. So we introduce a shifted time variable τ:

$$\tau = t - t_{i,n} \quad (11)$$

Equation (11) shows how much time that has passed since the last impact.
Where: $i \rightarrow$ ball (particle number)
$n \rightarrow$ bounce (impact number)
$T \rightarrow$ time interval (period of flight)
At the moment of the next impact**:**

$$t = t_{i,n_{+1}} \quad (12)$$

Substitute equation (12) into equation (10) we have:

$$T = t - t_{i,n} \quad (13)$$

Where: $t =$ current time, $t_{i,n} =$ last bounce time, $t_{i,n_{+1}} =$ next bounce time, $T =$ Time between bounces.
At impact, the elapsed time is equal to flight time.
Now factor T from equation (9), then the we obtain the trivial solution i.e., when the ball was at rest, $T = 0$. But solving for the non-trivial root solution we have:

$$T_{i,n}\left(v_{i,n}^+ - \frac{1}{2}gT_{i,n}\right) = 0 \quad (14)$$

Simplifying equation (14) further gives,

$$T = \frac{2v_i^+{}_{,n}}{g} \quad (15)$$

Equations (7), (10), and (15) together define an event-driven discrete update in which each impact instant generates a nonlinear state transition. Unlike continuously forced smooth oscillators, the present system evolves through successive discontinuous impact events, thereby forming a discrete non-smooth dynamical system governed by boundary-induced impulsive excitation (Barroso et al., 2009; Luo and Han, 1996; Bao et al., 2025). Defining the post-impact state of particle i at the n^{th} collision as $X_{i,n} = (t_{i,n}, v_i^+{}_{,n})$, the dynamics may be written in compact form as $X_{i,n+1} = \mathcal{F}(X_{i,n})$, where the nonlinear mapping $\mathcal{F}$ incorporates gravitational free-flight and boundary-induced impulsive excitation. The system therefore constitutes a non-smooth discrete dynamical system governed by impact events rather than continuous-time evolution. From equation (15), is the time of flight which is equal to the time going up plus time coming down. The gravity is constant, therefore;

$$T = t_{up} + t_{down} = \frac{v}{g} + \frac{v}{g} = \frac{2v}{g} \quad (16)$$

From our observation no physical contact occurs between the balls because the system behaves as a set of independent oscillators under gravity; thus, this is a multi-particle, non-interacting, 1D gravitational motion system. Hence we have,

$$r_i(t) = (0, y_i(t), 0) \quad (17)$$

Equation (17) shows that there is no inter-particle interaction, so

$$F_{ij} = 0 \; and \; y_i(t) \neq y_j(t), \;\; \forall_i \neq j \quad (18)$$

Equation (18) simply says the balls never touch each other at all time.

Consider equation (11) for temporally staggered motion for multiple balls where $N \; balls$ are launched at different times τ_i, then our equation (4) becomes :

$$y_i(t) = v_0(t - \tau_i) - \frac{1}{2} g(t - \tau_i)^2 \; , \; t \geq \tau_i \quad (19)$$

Equation (19) describes phase-shifted trajectories for multiple particles, consistent with temporally ordered motion observed in vibration-driven granular systems (Sonar et al., 2024; Watson et al., 2023).

It follows from equation (19) that no ball remains at the base long enough to overlap with another ball, thus; the base functions as a temporal separator and energy regulator. Therefore, if the arrival times are $t_1, t_2, \ldots, t_N \; with$:

$$|t_1 - t_j| > \tau_c \quad (20)$$

Where: τ_c is the contact time at the base, but it follows that

$$\tau_c \ll |t_i - t_j| \quad (21)$$

Equation (21) shows that no two balls are simultaneously at the base.

Each ball is relaunched with a characteristic velocity:

$$v_i^+ = v_0 + \Delta v_i \quad (22)$$

Equation (22) preserves the temporal spacing, therefore we have;

$$t_{i,n_{+1}} - t_{j,n_{+1}} = t_{i,n} - t_{j,n} \quad (23)$$

Equation (23) maintains separation at the base of the system, so there is no lateral motion, no crossing paths between particles, and each particle follows its own deterministic trajectory as tracks never intersect in time space as shown in equation (19). Therefore, this can be regarded as phase ordering. Equation (23) shows that temporal separation is preserved under successive updates, reflecting temporally ordered collective behavior consistent with structured granular transport systems (Sonar et al., 2024).

From equation (23), we have:

$$\Delta t_{ij}^{n+1} = \Delta t_{ij}^{n} \quad (24)$$

Although no explicit inter-particle forces are included Equation (18), the shared boundary induces an implicit coupling through impact timing. This results in an effective repulsive interaction in phase space: particles that approach synchronous impact experience differential velocity updates via Equation (7), leading to restoration of temporal separation. Hence, phase repulsion emerges as a boundary mediated dynamical effect rather than a direct force interaction. Equation (23) indicates that temporal ordering between particles is structurally preserved under successive impact updates. This persistence of staggered impact timing reflects the inherent stability of collision-free configurations under bounded excitation.

2.1.1 Periodic Boundary Excitation

Between successive impacts with the base, each particle undergoes vertical motion under gravity. The equation of motion for the *i*-th particle during free flight is given by

$$U(t) = Asin(\omega t + \emptyset) \quad (25)$$

Where A denotes the excitation amplitude, ω is the angular frequency, and $\emptyset$ is the phase. This formulation reflects the mechanical oscillation of the base and allows systematic analysis of its influence on particle dynamics.

From equation (25) we see that increasing A increases flight height and enhances phase separation, while excessive excitation leads to instability.

2.1.2 Stability of Temporally Ordered Motion

The stability of the particle trajectories is governed by the balance between dissipative losses and energy injection from the base excitation. In the absence of excitation ($A = 0$), repeated inelastic impacts lead to exponential decay of particle energy and eventual rest. When periodic excitation is introduced ($A > 0$), the rebound velocity is continuously replenished. Stable motion is achieved when the average injected energy balances dissipative losses. Within this regime, the discrete impact updates maintain temporal separation between particles, preventing synchronous impacts and sustaining ordered multi-particle motion:

$$\langle U(t) \rangle \approx (1 - e) v^- \quad (26)$$

Equation (26) represents the balance between energy injection and dissipation, a fundamental mechanism in vibro-impact systems under external excitation (García-Cid et al., 2015; Giusepponi et al., 2005). To further interpret stability, consider small perturbations in impact timing or velocity about the steady impact sequence. Under bounded excitation satisfying Eq. (27), successive impact updates do not amplify these perturbations, and the motion remains temporally ordered. Thus, the periodic impact motion persists under small disturbances. Under this condition, the system converges to a stable periodic orbit characterized by bounded flight heights and constant phase separation.
If the excitation amplitude is too small $(A \ll 1)$, dissipation dominates and motion decays. Conversely, excessive excitation $A \gg 1$, may induce irregular trajectories and destabilize phase ordering. Therefore, stable collision-free dynamics occur within a bounded excitation regime:

$$Amin < A < Amax \tag{27}$$

Equation (27) defines the bounded excitation regime required for stable operation, consistent with stability conditions in vibration-driven and non-autonomous systems (Lampart and Zapoměl, 2016; Torres and Núñez, 2009). To further clarify the stability mechanism, consider a small perturbation in the post-impact velocity about a periodic impact sequence. Let $v_i^+{}_{,n} = v^* + \delta v_{i,n}$, where v^* denotes the steady-state post-impact velocity and $\delta v_{i,n}$ is a small deviation.
Substituting into the discrete update defined by Equations (7), (10), and (15) and retaining first-order terms yields a linearized relation of the form $\delta v_{i,n+1} = e\delta v_{i,n} + \frac{\partial U}{\partial t} \Big| t = t_{i,n}$.

Since the restitution coefficient satisfies $0 < e < 1$, dissipative effects naturally suppress the amplification of small perturbations between successive impacts. Under bounded excitation, the timing-dependent velocity updates remain finite and therefore do not destabilize the staggered impact sequence. Consequently, small disturbances gradually decay with repeated impacts, ensuring preservation of temporal ordering and local stability of the collision-free configuration. Equation (27) shows the regime that defines the operational window of the base platform. The impact dynamics therefore constitute a non-smooth, event-driven update process in which stable temporal organization emerges from the balance between gravitational flight and boundary-mediated excitation.

3. Results and Discussion

The results obtained in this study confirm the validity of the proposed collision-free multi-particle model and demonstrate the effectiveness of boundary-induced regulation. The persistence of temporal ordering across increasing particle populations indicates that the collision-free configuration corresponds to an invariant manifold of the discrete impact map. Numerical evidence suggests that this manifold remains stable under bounded excitation, supporting the theoretical prediction of phase-preserving dynamics derived in Section 3. The single-particle analysis shows that, in the absence of external excitation, successive impacts lead to progressive energy dissipation and decreasing flight height. This behavior is consistent with the restitution-based rebound law and validates the fundamental assumptions of the model.

For multiple particles, the numerical simulations reveal persistent phase separation and stable trajectory ordering. The height–time plots indicate that individual particles follow periodic parabolic paths with preserved temporal offsets. This temporal ordering prevents inter-particle collisions and ensures long-term dynamical stability. When the number of particles is increased from five to one hundred, the system maintains bounded oscillations and ordered motion. No trajectory overlap or clustering is observed, demonstrating the scalability of the proposed framework. These results confirm that collision-free behavior is sustained even at high particle densities. The introduction of periodic base excitation significantly enhances system stability. The excitation term compensates for dissipative losses and maintains finite flight heights over extended time intervals. Within an appropriate excitation regime, the system converges to stable periodic orbits characterized by constant phase spacing and controlled energy levels. Overall, the agreement between analytical predictions and numerical simulations confirms that boundary-mediated excitation is the primary mechanism governing phase preservation and collision suppression in the proposed system.

3.1 Simulation Parameters and Dataset

All numerical simulations were performed using a fourth-order Runge-Kutta integration scheme implemented in MATLAB. A sufficiently small fixed time step was selected to ensure numerical convergence and stability of the impact trajectories. Transient dynamics were discarded prior to data acquisition in order to isolate steady-state behavior. The simulation dataset comprised 200 randomized parameter realizations spanning stable, transitional, and weakly unstable operating regimes, thereby enabling systematic evaluation of model robustness and parameter sensitivity.

Table 1. Simulation Parameters

Parameter	Symbol	Value	Unit	Description
Gravitational acceleration	g	9.81	m s^{-2}	Acceleration due to gravity
Restitution coefficient	E	0.90	-	Impact dissipation parameter
Excitation amplitude	A	1.20	m s^{-1}	Base excitation strength
Excitation frequency	Ω	2π	rad s^{-1}	Angular frequency of excitation
Phase shift	Φ	0.0	rad	Initial excitation phase
Initial velocity	v_0	5.0	m s^{-1}	Initial launch velocity
Time step	Δt	0.001	S	Numerical integration step
Simulation time	$Tmax$	12	S	Total simulation duration
Number of particles	N	1–100	-	Particle population

The simulation code is available from the corresponding author upon reasonable request.

To examine parameter sensitivity, 200 randomized samples were generated within physically realistic ranges based on the experimental configuration and baseline simulation values. Extending the analysis to multi-particle configurations, Figure 7 depicts the trajectories of twenty particles with distinct phase shifts. The preserved temporal separation and bounded oscillatory behavior demonstrate the effectiveness of boundary-mediated excitation in maintaining ordered motion and preventing simultaneous impacts. To further assess model robustness, Figure 8 presents the sensitivity of maximum rebound height to variations in the coefficient of restitution. The narrow distribution of data points indicates limited dependence on moderate parameter fluctuations, thereby confirming the stability of the proposed framework under realistic operating uncertainties.

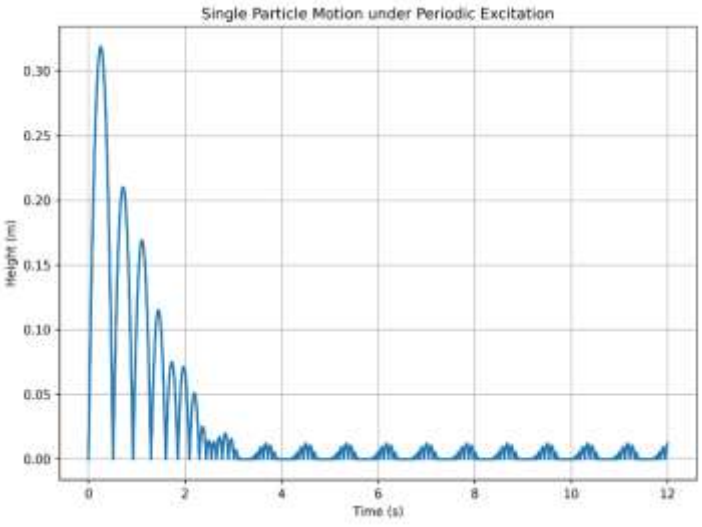

Figure 1**: Single Ball Motion**

Figure 1 shows the height–time response of a single particle subjected to periodic base excitation. The motion consists of successive parabolic flights separated by inelastic impacts. An initial transient phase characterized by large rebound heights is observed, followed by progressive amplitude decay due to energy dissipation. At later times, the system converges to a bounded oscillatory regime, indicating a balance between dissipative losses and external excitation. This behavior confirms the validity of the proposed single-particle dynamic model. The observed transition from large transient rebounds to bounded oscillatory motion reflects the gradual balance established between excitation-induced

energy injection and restitution-based dissipation. This behavior is consistent with stable periodic bouncing regimes previously reported in classical impact oscillator studies by Holmes and Luo. The convergence toward bounded trajectories further confirms that the excitation mechanism maintains long-term dynamic stability while preventing unbounded energy growth. From an engineering perspective, such regulated periodic motion is desirable in vibration-assisted transport systems requiring predictable and repeatable particle trajectories.

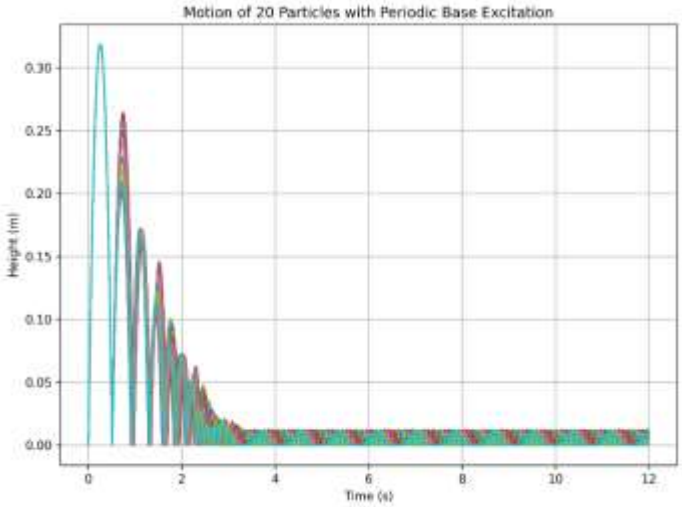

Figure 2: Motion of 20 Balls

Figure 2 presents the trajectories of twenty particles with distinct phase shifts. During the early stage, all particles exhibit high-amplitude bouncing similar to the single-particle case. As the system evolves, rebound heights decrease and converge toward a narrow oscillatory band. The preserved temporal separation between trajectories prevents simultaneous impacts and suppresses inter-particle collisions. These results demonstrate stable and ordered dynamics in moderately sized multi-particle systems. The preserved temporal offsets between adjacent trajectories demonstrate that the structured vibrating boundary acts as an effective phase regulator. Although no direct inter-particle forces are introduced, the shared excitation mechanism dynamically maintains staggered impact timing and suppresses clustering. Similar phase-ordering phenomena have been observed in structured granular transport systems subjected to controlled vibration forcing. The present results extend these observations by establishing a discrete dynamical explanation for collision suppression through boundary-mediated synchronization.

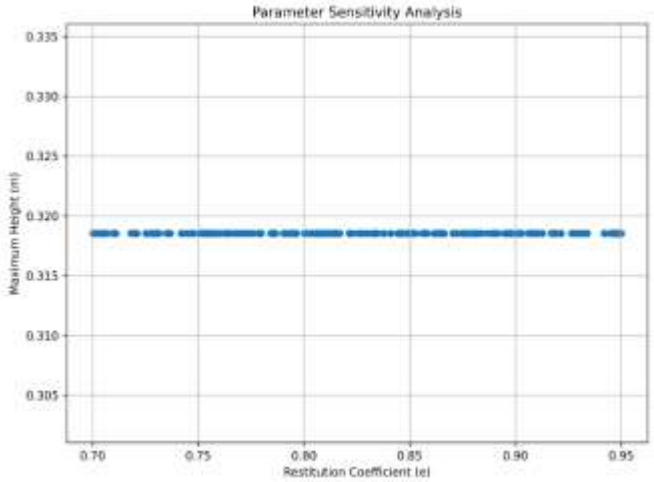

Figure 3: **Parameter Sensitivity Analysis**

Figure 3 shows the relationship between the coefficient of restitution and the maximum rebound height obtained from 200 randomized parameter samples. The data points form a narrow horizontal band, indicating limited sensitivity of the system response to moderate variations in restitution. This result highlights the stabilizing effect of periodic base excitation and confirms the robustness of the model under parameter uncertainty.

The weak sensitivity of rebound height to moderate restitution variations indicates that the proposed framework possesses strong parametric robustness. This stability arises because the excitation-induced phase regulation compensates for small dissipative fluctuations, thereby preserving bounded impact dynamics over a wide operating range. Such robustness is particularly important in practical engineering systems where material properties and environmental conditions may vary during operation.

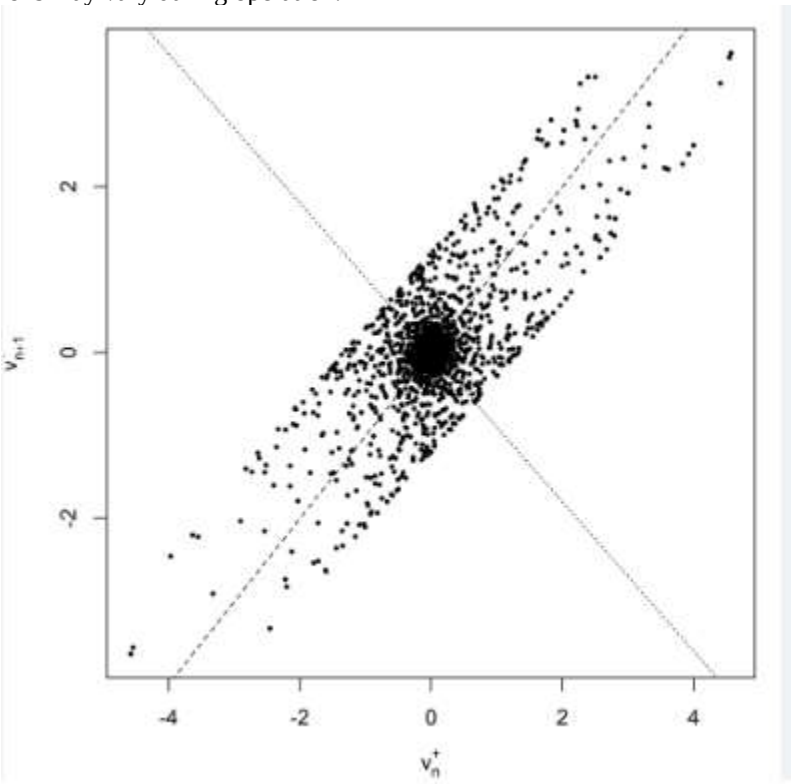

Figure 4: Discrete impact return map

The discrete return map in Fig. 4 reveals two symmetric attracting branches separated from the identity line, indicating the emergence of a stable period-2 impact orbit. The dominant slope of the map is governed by the restitution coefficient, satisfying $|e| < 1$, which induces contraction in velocity space. Iterates initiated from diverse initial conditions converge toward the attracting branches, confirming local stability of the staggered impact sequence. No stable fixed point corresponding to synchronous impacts is observed in the explored parameter regime. The bounded structure of the map demonstrates that the system evolves toward a stable non-smooth discrete dynamical regime under bounded excitation. The emergence of two attracting branches indicates the formation of a stable period-two non-smooth orbit within the discrete impact map. The contraction induced by the restitution coefficient ensures convergence of nearby trajectories toward the attracting manifold, while the absence of stable synchronous fixed points confirms the instability of simultaneous impacts. This behavior supports the interpretation that collision-free operation represents a dynamically preferred configuration of the impact system under bounded excitation.

3.2. Experimental Setup

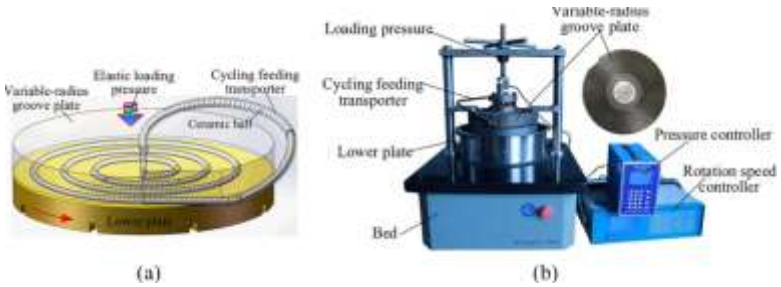

Figure 5: Overall Experimental Setup

Figure 5 shows the complete experimental arrangement used to investigate collision-free multi-particle dynamics under impulsive excitation. The system consists of a compact vibratory platform mounted on a rigid support frame, with a cylindrical housing enclosing the excitation mechanism. A radially structured top plate is fixed at the upper surface of the device, providing guided motion paths for the particles. The excitation unit, embedded within the housing, generates vertical vibration of the platform, while the surrounding frame minimizes external disturbances. The figure provides an overview of the mechanical layout and spatial configuration of the experimental apparatus.

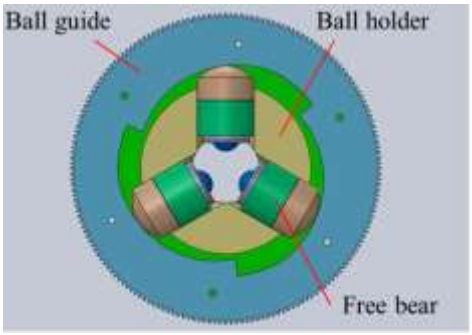

Figure 6: Radially Structured Platform Surface

Figure 6 illustrates a detailed view of the top plate of the vibratory platform. The surface is machined with uniformly spaced radial grooves extending from the center toward the perimeter, forming a star-shaped geometry. These grooves constrain lateral particle motion and guide individual particles along predefined trajectories. The structured surface plays a critical role in regulating particle dynamics by promoting phase separation and reducing the likelihood of inter-particle collisions during repeated impacts.

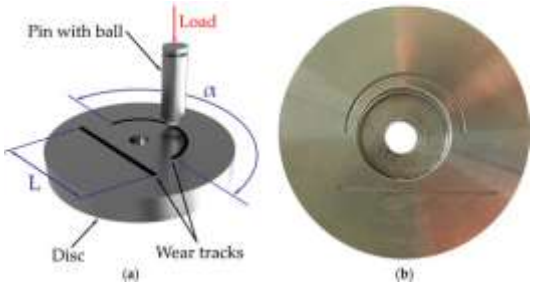

Figure 7: Particle Motion Observation and Recording Arrangement

Figure 7 presents the experimental arrangement used for observing and recording particle motion. A high-speed camera (or smartphone camera operating at high frame rates) is positioned above the platform and aligned normal to the surface to capture vertical particle trajectories with minimal perspective distortion. A calibrated reference scale is placed within the field of view to enable conversion of pixel measurements into physical dimensions. This setup allows accurate extraction of displacement, impact timing, and rebound characteristics from recorded video data.

3.2.1 Description of the Vibratory Platform

3.2.2 Mechanical and Geometric Characteristics

The principal geometric and mechanical parameters of the experimental platform are summarized in Table 2.

Table 2. Platform Specifications

Parameter	Symbol	Value	Unit
Platform diameter	D	180	mm
Platform height	H	85	mm
Groove number	Ng	24	–
Groove depth	dg	2.0	mm
Material	–	Aluminum alloy	–
Excitation type	–	Internal eccentric motor	–
Power supply	–	DC adapter (12 V)	–

These parameters were selected to ensure stable excitation and repeatable particle motion under laboratory conditions.

The experimental investigations were performed using a compact, self-contained vibratory impact platform, consistent with the system demonstrated in the accompanying video. The apparatus consists of a cylindrical aluminum housing containing an integrated excitation mechanism and a detachable radially structured top plate. The upper surface is machined with uniformly spaced radial grooves extending from the center to the perimeter, forming a star-shaped pattern. These grooves constrain lateral particle motion and guide the trajectories of spherical particles along predefined paths, thereby promoting phase separation and suppressing inter-particle collisions. The platform operates predominantly in the vertical direction and generates impulsive excitation through internal vibration. The excitation mechanism consists of a DC motor coupled to an eccentric rotating mass, which produces periodic vertical acceleration of the top plate and induces repeated particle rebounds.

3.2.3 Test Particles.

Polished stainless-steel spheres were used as test particles to ensure uniform mass distribution and consistent surface properties. The particle specifications are presented in Table 3.

Table 3. Particle Properties

Parameter	Symbol	Value	Unit
Diameter	dp	8–10	mm
Mass	m	3.5–4.5	g
Material	–	Stainless steel	–

Before each experiment, the particles were cleaned with ethanol to remove dust and oil residues that could influence impact behavior.

3.2.4 Excitation Control and Calibration

The excitation system was powered by a variable-voltage DC supply connected to the internal motor. By adjusting the input voltage, the rotational speed of the eccentric mass was regulated, thereby controlling the vibration frequency and amplitude of the platform. The excitation frequency was measured using a digital tachometer, while vibration amplitude was estimated through accelerometer measurements and video-based displacement analysis. Calibration tests were conducted prior to experimentation to establish the relationship between input voltage and excitation characteristics. The operating frequency range was approximately 8–35 Hz, corresponding to stable operating conditions observed during preliminary tests.

3.2.5 Motion Recording and Measurement

Particle motion was recorded using a high-speed smartphone camera mounted on a rigid stand above the platform. The camera was aligned normal to the surface to minimize perspective distortion.

Recording parameters were as follows:

Frame rate: 120–240 fps

Resolution: 1920 × 1080 pixels

Recording duration: 30–60 s

A calibrated reference scale was placed within the camera field of view to enable conversion from pixel coordinates to physical distances.

Recorded videos were processed using digital image analysis and particle tracking software to extract displacement, velocity, and impact timing information.

3.2.6 Experimental Procedure

Experiments were conducted following a standardized protocol to ensure repeatability:

A specified number of steel spheres (N = 1, 5, 20, and up to 50) was placed within selected radial grooves.

The excitation voltage was adjusted to obtain the desired vibration level.

The platform was operated for 20 s to reach steady-state conditions.

Video recording was initiated and continued for 40 s.

Each test was repeated at least four times under identical conditions.

Recorded data were stored and processed for subsequent analysis.

All experiments were performed on a vibration-isolated laboratory table at room temperature (25 ± 2 °C).

3.2.7 Data Processing and Analysis

From the recorded video data, the vertical displacement of each particle was extracted using frame-by-frame tracking. Impact instants were identified from abrupt changes in velocity direction.

The following quantities were determined:

Flight time between successive impacts
Maximum rebound height
Impact velocity
Phase difference between particles
Temporal separation at the base
Mean values and standard deviations were computed over repeated trials to quantify experimental uncertainty. The experimentally obtained results were compared with theoretical predictions to assess model accuracy.

3.2.8 Repeatability and Uncertainty Assessment

To evaluate experimental repeatability, selected test cases were repeated on different days. The coefficient of variation of rebound height and flight time was found to be below 8% for all stable operating conditions.
Measurement uncertainties arising from camera resolution, calibration error, and tracking accuracy were quantified and incorporated into the validation analysis. Temporal synchronization between the excitation mechanism and particle motion was achieved through frame-by-frame alignment of recorded trajectories with the measured excitation frequency. Spatial calibration was performed using a fixed reference scale positioned within the camera field of view prior to experimentation. Uncertainty contributions arising from image resolution, frame discretization, particle tracking accuracy, and calibration error were quantified using repeated measurements. The combined uncertainty in rebound height remained below ±5%, while the uncertainty in impact timing remained below one video frame interval throughout all stable operating conditions.

3.2.9 Experimental Validation

To evaluate the accuracy and reliability of the proposed analytical model, experimental measurements obtained from the vibratory platform were systematically compared with theoretical predictions derived from the governing equations. Validation was carried out using high-speed video recordings of particle motion under controlled excitation conditions. The validation focused on key dynamical parameters that characterize system performance, namely: The validation focused on key dynamical parameters characterizing system performance, namely flight time between successive impacts, maximum rebound height, impact velocity, phase separation between adjacent particles, and temporal separation at the base. These quantities directly reflect the stability, repeatability, and collision-free behavior of the system.

3.3 Comparison Between Theoretical and Experimental Results

To further assess model robustness, Figure 8 presents the sensitivity of maximum rebound height to variations in the coefficient of restitution. The narrow distribution of data points indicates limited dependence on moderate parameter fluctuations, thereby confirming the stability of the proposed framework under realistic operating uncertainties.

3.3.1 Quantitative Error Analysis

To quantify the agreement between theory and experiment, the relative error in rebound height was computed using:

$$Error(\%) = \frac{|H_{exp-H_{th}}|}{H_{exp}} \times 100$$

where H_{exp} and H_{th} denote the experimental and theoretical maximum rebound heights, respectively.
Table 4 summarizes the average errors obtained for representative test cases.

Table 4. Comparison of Experimental and Theoretical Results

Case	Number of Particles	Mean Height Error (%)	Mean Period Error (%)
A	1	3.8	2.9
B	5	5.2	4.1
C	20	6.4	5.3
D	50	7.1	6.0

The results indicate that the prediction error remains below 8% for all investigated configurations, demonstrating satisfactory agreement between the analytical model and experimental measurements.

3.3.2 Validation of Phase Separation and Collision Suppression

A principal objective of the proposed framework is the maintenance of phase separation and prevention of inter-particle collisions. This behavior was examined by analyzing temporal spacing between successive particle impacts at the base.

Let t_i^n denote the time of the nth impact of particle i. The minimum temporal separation between adjacent particles was computed as:

$\Delta t_{min} = \min\left|t_i^n - t_j^n\right|, i \neq j$

Experimental results showed that Δt_{min} remained strictly positive throughout the observation period for all stable operating conditions, confirming the absence of simultaneous impacts. Visual inspection of video recordings further verified that no direct inter-particle contacts occurred during steady-state operation, even for particle populations exceeding fifty. These findings validate the model prediction that boundary-mediated excitation preserves temporal ordering and suppresses collisions.

3.3.3 Repeatability and Reliability Assessment

Selected experiments were repeated on different days under identical conditions to evaluate repeatability. The coefficient of variation of rebound height and flight time was found to be less than 8% in all cases, indicating good experimental consistency. These results confirm experimental repeatability and model reliability.

4. Results and Discussion

The comparison between theoretical predictions and experimental measurements demonstrates strong quantitative agreement across all tested configurations. In particular, the relative error in rebound height remains below 8%, indicating that the proposed model accurately captures the dominant dynamics of the system. Furthermore, the model successfully reproduces the observed phase separation and absence of inter-particle collisions. Experimental observations confirm that the minimum temporal separation between particle impacts remains strictly positive throughout the operation, validating the predicted collision-free regime. These results establish that boundary-mediated excitation provides a reliable mechanism for sustaining stable, collision-free multi-particle motion, with both qualitative and quantitative agreement between theory and experiment. The present formulation neglects several secondary physical effects, including rotational dynamics, finite contact duration, tangential friction, aerodynamic drag, and surface roughness variations. These simplifications were introduced to preserve analytical tractability and isolate the dominant mechanisms governing boundary-induced phase regulation. Although such effects may slightly modify detailed rebound characteristics in practical systems, the experimental results demonstrate that the proposed model accurately captures the primary synchronization, stability, and collision-suppression behavior observed under laboratory operating conditions.

5. Conclusion and Recommendations

The system admits a discrete non-smooth dynamical description in which staggered impact timing emerges as a stable attracting configuration of the impact map. Synchronous impacts are dynamically unstable under excitation-induced perturbations, whereas temporally separated trajectories form an invariant structure preserved under successive updates. The collision-free multi-particle state therefore arises not from direct inter-particle forces but from boundary-mediated timing regulation encoded in the discrete impact dynamics. This mechanism establishes phase ordering as an emergent property of impulsively excited non-smooth systems. The present framework extends classical single-particle vibro-impact models to a multi-particle setting and provides a dynamical interpretation of collision suppression through boundary-induced phase organization. These results situate the system within the broader class of impact-driven nonlinear dynamical systems and suggest potential applications in vibration-assisted transport and controlled particulate manipulation. The proposed framework provides a theoretical basis for the development of vibration-assisted transport, sorting, and particulate handling systems in which trajectory regulation and collision suppression are essential. More broadly, the demonstrated emergence of collective ordering through shared-boundary excitation suggests new possibilities for passive synchronization and control in impact-driven nonlinear engineering systems.

Declaration of Generative AI and AI-assisted technologies in the writing process

During the preparation of this work, the author used ChatGPT (OpenAI) to assist in language refinement, grammatical improvement, manuscript organization, and response preparation during the peer-review revision process. After using this tool, the author carefully reviewed, edited, and validated the content as needed and takes full responsibility for the content of the publication.

References

Adachi, M., Shirode, K., Yamato, S., Tanaka, K., Kanamori, H.: Granular vibration pumping system for handling and characterizing particulate materials. Rev. Sci. Instrum. 95, 055102 (2024). https://doi.org/10.1063/5.0202652

Adhikari, R., Mishra, S., Patel, K.: Granular vibration pumping and particulate transport applications. Proc. ASME Int. Mech. Eng. Congr. Expo. (2024). https://doi.org/10.52202/078357-0180

Bao, L., Kuske, R., Yurchenko, D., Belykh, I.: Computer-assisted global analysis for vibro-impact dynamics: a reduced smooth maps approach. SIAM J. Appl. Dyn. Syst. 24, 1891–1944 (2025). https://doi.org/10.1137/24M1652763

Barroso, J.J., Carneiro, M.V., Macau, E.E.N., Silva, A.: Bouncing ball problem: stability of the periodic modes. Phys. Rev. E 79, 026206 (2009). https://doi.org/10.1103/PhysRevE.79.026206

Chastaing, J.-Y., Bertin, E., Géminard, J.-C.: Dynamics of the bouncing ball. Am. J. Phys. 83, 518–526 (2015). https://doi.org/10.1119/1.4890571

Dekemele, K., Habib, G.: Softening versus hardening nonlinear energy sinks: forced vibration control and isolated resonance curves. Nonlinear Dyn. 113, 19179–19198 (2025). https://doi.org/10.1007/s11071-025-11164-6

Dorbolo, S., Volfson, D., Tsimring, L., Kudrolli, A.: Dynamics of a bouncing dimer. Phys. Rev. Lett. 95, 044101 (2005). https://doi.org/10.1103/PhysRevLett.95.044101

El Banna, R., Liutkauskienė, K., Česnavičius, R., Lendraitis, M., Dagilis, M., Kilikevičius, S.: Vibrational transport of granular materials achieved by dynamic dry friction manipulations. Appl. Sci. 16, 630 (2026). https://doi.org/10.3390/app16020630

Fritzkowski, P., Awrejcewicz, J.: Near-resonant dynamics, period-doubling and chaos of 3-DOF vibro-impact system. Nonlinear Dyn. 104, 2543–2564 (2021). https://doi.org/10.1007/s11071-021-06948-6

García-Cid, A., Puglisi, A., Trizac, E., Visco, P.: Statistics of injected power on a bouncing ball subjected to a random piston. Phys. Rev. E 92, 032915 (2015). https://doi.org/10.1103/PhysRevE.92.032915

Giusepponi, S., Marchesoni, F.: The chattering dynamics of an ideal bouncing ball. Europhys. Lett. 64, 36–42 (2003). https://doi.org/10.1209/epl/i2003-10089-0

Giusepponi, S., Marchesoni, F., Borromeo, M.: Randomness in the bouncing ball dynamics. Physica A 351, 142–158 (2005). https://doi.org/10.1016/j.physa.2004.12.016

Gong, C., Fang, X., Cheng, L.: Multi-state dynamics and model similarity of a vibro-impact nonlinear system. Int. J. Non-Linear Mech. 163, 104765 (2024). https://doi.org/10.1016/j.ijnonlinmec.2024.104765

Gzal, M.O., Gendelman, O.V., Bergman, L.A., Vakakis, A.F.: How internal vibro-impact nonlinearities yield enhanced vibration mitigation. Nonlinear Dyn. 112, 17683–17708 (2024). https://doi.org/10.1007/s11071-024-09902-3

Herisanu, N., Marinca, B., Cveticanin, L., Marinca, V.: Analysis of the vibro-impact nonlinear damped and forced oscillator near primary resonance. Mathematics 11, 2194 (2023). https://doi.org/10.3390/math11092194

Holmes, P.J.: The dynamics of repeated impacts with a sinusoidally vibrating table. J. Sound Vib. 84, 173–189 (1982). https://doi.org/10.1016/0022-460X(82)90215-2

Lampart, M., Zapoměl, J.: Dynamical properties of a non-autonomous bouncing ball model forced by non-harmonic excitation. Math. Methods Appl. Sci. 39, 4923–4929 (2016). https://doi.org/10.1002/mma.4186

Li, H., Li, S., Zhang, Z., Xiong, H., Ding, Q.: Effectiveness of vibro-impact nonlinear energy sinks for vibration suppression of beams under traveling loads. Mech. Syst. Signal Process. 223, 111861 (2025). https://doi.org/10.1016/j.ymssp.2024.111861

Liu, R., Kuske, R., Yurchenko, D.: Maps unlock dynamics of targeted energy transfer via vibro-impact nonlinear energy sinks. Mech. Syst. Signal Process. 191, 110158 (2023). https://doi.org/10.1016/j.ymssp.2023.110158

Luck, J.M., Mehta, A.: Bouncing ball with a finite restitution: chattering, locking and chaos. Phys. Rev. E 48, 3988–3997 (1993). https://doi.org/10.1103/PhysRevE.48.3988

Luo, A.C.J., Han, R.P.S.: The dynamics of a bouncing ball with a sinusoidally vibrating table revisited. Nonlinear Dyn. 10, 1–18 (1996). https://doi.org/10.1007/BF00114795

Luo, A.C.J., Zhu, Y.: Periodic motions with impact chatters in an impact Duffing oscillator. Chaos 34, 053124 (2024). https://doi.org/10.1063/5.0210693

Pagano, D., Perna, G., De Angelis, M., Andreaus, U.: Nonlinear dynamic response of vibro-impact systems subjected to harmonic ground motion under uncertainty in the gap size. Int. J. Non-Linear Mech. 165, 104816 (2024). https://doi.org/10.1016/j.ijnonlinmec.2024.104816

Sonar, P., Kumar, A., Das, S., Mahadevan, L.: Granular flows over normally vibrated inclined bases. Phys. Rev. Fluids 9, 124304 (2024). https://doi.org/10.1103/PhysRevFluids.9.124304

Torres, P.J., Núñez, J.A.: Stabilization by vertical vibrations. Math. Methods Appl. Sci. 32, 1137–1152 (2009). https://doi.org/10.1002/mma.1083

Veltman, Y., Gzal, M., Gendelman, O.V.: Intermodal targeted energy transfer in two dimensions. Nonlinear Dyn. 113, 14245–14263 (2025). https://doi.org/10.1007/s11071-025-10909-7

Watson, P., Vincent-Bonnieu, S., Lappa, M.: Fluidization and transport of vibrated granular matter: a review of landmark and recent contributions. Fluid Dyn. Mater. Process. 20, 1–29 (2023). https://doi.org/10.32604/fdmp.2023.029280

Weidemann, T., Bergman, L.A., Vakakis, A.F., et al.: Energy transfer and localization in a forced cyclic chain of oscillators with vibro-impact nonlinear energy sinks. Nonlinear Dyn. 113, 14319–14360 (2025). https://doi.org/10.1007/s11071-025-10928-4

Xie, J., Li, Y., Wang, Z.: Dynamical analysis of vibro-impact systems with fractional-order damping. Math. Methods Appl. Sci. 45, 11054–11072 (2022). https://doi.org/10.1002/mma.8357

Yan, Y., Páez Chávez, J., Shen, J.: Dynamics of the vibro-impact capsule robot with a von Mises truss. Nonlinear Dyn. 113, 11047–11067 (2025). https://doi.org/10.1007/s11071-024-10653-4

Youssef, B., Karoui, A.Y., Leine, R.I.: Asymmetric vibro-impact nonlinear energy sink with dry friction: an impact map approach. Nonlinear Dyn. (2025). https://doi.org/10.1007/s11071-025-11692-1

Zhang, J., Yin, S., Guo, B., Liu, Y.: Vibro-impact dynamics of an experimental rig with two-sided constraint and bidirectional drift. J. Sound Vib. 571, 118021 (2024). https://doi.org/10.1016/j.jsv.2023.118021